J Solid State Electrochem (2008) 12:1579–1587
DOI 10.1007/s10008-008-0523-5

ORIGINAL PAPER

pH-sensing properties of PbO_2 thin film electrodeposited on carbon ceramic electrode

H. Razmi · H. Heidari · Es. Habibi

Received: 26 December 2007 / Revised: 25 January 2008 / Accepted: 26 January 2008 / Published online: 20 February 2008

Abstract In this paper, a new highly sensitive potentiometric pH electrode is proposed based on the solid-state PbO_2 film electrodeposited on carbon ceramic electrode (CCE). Two different crystal structures of PbO_2, α and β were examined and the similar results were obtained. Moreover, the experimental results obtained for the proposed pH sensor and a conventional glass pH electrode were in good agreement. The electromotive force (emf) signal between the pH-sensitive PbO_2-coated CCE and SCE reference electrode was linear over the pH range of 1.5–12.5. Near-Nernstian slopes of −64.82 and −57.85 mV/pH unit were obtained for α- and β-PbO_2 electrodes, respectively. The interferences of some mono-valence and multi-valence ions on potentiometric response of the sensor were studied. The proposed pH sensor displayed high ion selectivity with respect to K^+, Na^+, Ca^{2+}, and Li^+, with log $K^{pot}_{H,M}$ values around −12 and has a working lifetime of about 30 days. Key parameters important for the pH sensor performance, including kind of PbO_2 film, selectivity, response time, stability, and reproducibility, have been characterized. The proposed electrode showed a good efficiency for direct pH-metry after calibration and pH-metric titrations without calibration step. The response time was about 1 s in acidic medium and less than 30 s in alkaline solutions. The pH values of complex matrix samples such as fruit juices measured by the proposed sensor and a conventional glass pH electrode were in good agreement.

H. Razmi (✉) · H. Heidari · Es. Habibi
Electrochemistry Research Lab., Faculty of Sciences,
Azarbaijan University of Tarbiat Moallem,
P.O. Box 53714-161, Tabriz, Iran
e-mail: h.razmi@azaruniv.edu

Keywords Carbon ceramic electrode · Sol–gel · Nernstian slope · Lead dioxide · pH sensor · Modified electrode

Introduction

The first uses of the glass pH electrode as an ion-selective electrode (ISE) date from the beginning of the 20th century [1]. Conventional pH electrodes are usually based on a pH-sensitive glass membrane. The glass bulb pH electrode is a well-established tool in the pH measurement, especially in crucial areas such as agricultural chemistry, food chemistry, pharmaceutics industry, and human health. The interest in measuring and controlling the pH of fluids, or organisms in chemistry, biomedics, cosmetics, food, and environmental areas is very important from a practical point of view [2–4]. The glass electrode has proved to be the most popular electrode owing to its high selectivity, reliability, and convenience of use. However, a number of significant disadvantages of the glass pH electrode have also been recognized, such as higher cost, high impedance and temperature instability, large size, the need for internal solution limiting its use only in a vertical position, fragility of the glass, and the difficulty of miniaturization [5]. In addition, a normal glass electrode needs a long time to reform a hydrate layer before use. There has been considerable interest in designing non-glass pH sensors to overcome some of the above mentioned limitations of the glass electrode. In attempts to improve the pH sensor, chemically modified potentiometric electrodes have gained considerable attention, as they show many important advances [6–11].

Considering pH sensor technology, it is a challenge to obtain cheaper and more accurate sensors. In recent years,

numerous efforts have been directed towards the development of optical fiber pH sensors [12–14]. Optical fiber pH sensors are based on pH-induced reversible changes in optical or spectroscopic properties such as the absorbance, reflectance, transmittance, fluorescence, energy transfer, etc. Their principal advantage over other types of sensors, as the electronics, is the immunity to electromagnetic interference, small size, explosion proof, remote sensing, possibility of multiplexing, etc. The main component in an optical fiber sensor is a pH-sensitive dye deposited onto the tips or extremes of an optical fiber.

One of the classical potentiometric pH electrodes is provided based on quinhydrone, a combination of hydroquinone and quinine, and has found wide application in pH-sensing devices [15–17]. The pH-sensing characteristics of polypyrrole thin film were improved when the corresponding monomers were functionalized with hydroquinone [18]. It has been shown in earlier studies [19], that composite electrodes based on quinhydrone are useful for calibration-free measurements in solutions with pH values up to 8.5. These electrodes have the same properties as a conventional quinhydrone electrode but, additionally, they can be used in emulsions and they can be produced as very robust electrodes. The theory of the potential dependence of the quinhydrone electrode is described in literature [20]. Quinhydrone composite as well as graphite/quinhydrone composite was used to instruction of a non-glass pH electrode and showed good response to pH changes without calibration step [21–22].

Recently, electrosynthesized polymers are considered to be good candidates as pH sensors due to the fact that they are strongly bonded to the electrode surfaces during the electropolymerization step. The polyethyleneimine (PEI)- and polypropyleneimine (PPI)-modified platinum electrodes were prepared by electropolymerization method [23]. The potentiometric responses of these electrodes to pH changes appeared linear, reversible, and stable in time thanks to the amino groups present in the polymer backbone. In addition, the pH-sensing properties of electrosynthesized polypyrrole, poly(*p*-phenylenediamine), and polyaniline-modified platinum electrodes were reported [11]. Nyholm and Peter found that the electroactivity of the polyaniline redox centers is affected by the oxidation status of the polyaniline films rather than by the medium pH [24]. Karyakin et al. used a dip-coating technique for the electroless deposition of thick polyaniline films onto glassy carbon and screen-printed electrodes in developing biosensors where polyaniline was utilized as a pH transducer to determine urea [25] and glucose [26]. On the basis of the characteristics of high conductivity, ion-exchange capability, and the doping–undoping mechanism, polyaniline-modified electrodes have been developed as detectors or sensors for pH [25, 27–28], metallic ions [29], organic and biological molecules [30–32], and as immunosensors [33].

Another alternative to glass bulb electrodes is to use structures with metal oxide as the active component. A pH response has been observed for several metal oxides. These include IrO_2 [34–37], RuO_2 [38–42], OsO_2, Ta_2O_5, TiO_2, PtO_2, PdO, ZrO_2 [43, 44], PbO_2 [45], SnO_2, [46], molybdenum oxide [47], MnO [48–49], nanosized cobalt oxide [50], etc. Of these oxides, those based upon the platinum group metals are most commonly used, in particular, the dioxides of iridium, platinum, and ruthenium. Methods of construction used to manufacture metal oxide pH sensors vary according to the oxide and the application to which they are to be applied to. Manufacturing methods include thermal or anodic oxidation of the metal, decomposition of a metal salt onto a back contact, pressed oxide pellets, and holding the oxide in an inert matrix [41].

The employment of sol–gel chemistry to produce carbon-based conducting matrixes has received increasing interest in recent years [51–55]. The use of this type of procedure to find alternative materials to the ones typically used in solid electrodes must be explained in terms of a series of characteristics that points them out as plausible options. Advantageous features include high conductivity, relative chemical inertness, wide operational voltage window, good mechanical properties, physical rigidity, renewable surface, amenable chemical or biological modification, and stability in various solvents [56, 57]. In addition, the procedure developed for the fabrication of the electrodes is easy; by simply adding graphite to the precursor's solution, conductivity is conferred to it and the mixture is readily malleable, so that virtually any configuration can be obtained. Furthermore, there is also the opportunity to tailor the structures by controlling the chemistry of the sol–gel process, thus yielding materials with very different properties [58].

In this report, we demonstrate the utility of carbon ceramic electrode (CCE) as a novel substrate for electrodeposition of α- or β-PbO_2 films and application of the resulting modified electrodes as a potentiometric sensor for measuring of the solutions pH for first time. The modified CCE showed excellent results in acid–base titrations and measuring of pH in some real samples.

Experimental

Chemicals Methyltrimethoxysilane (MTMOS) was purchased from Merck and used without any further purification. Graphite powder of high purity was from Merck. The phosphate buffer solutions (PBS) (0.1 M) were prepared from H_3PO_4, KH_2PO_4, and K_2HPO_4. The pH of buffer solutions was adjusted by HNO_3 and KOH solutions. $Pb(NO_3)_2$, Pb

$(CH_3COO)_2$, and other reagents were of analytical grade from Merck.

Instrumentation AUTOLAB PGSTAT-100 (potentiostat/galvanostat) equipped with an USB electrochemical interface and driven GEPS software was used for electrochemical experiments. A three-electrode system and a personal computer for data storage and processing were used for preparation of α- or β-PbO_2 films. The utilized three-electrode system was composed of a saturated calomel electrode (SCE) as the reference electrode, a platinum wire as the auxiliary electrode and the α- or β-PbO_2-modified carbon ceramic electrodes (geometric surface area of 0.119 cm^2) as working electrode were employed for the electrochemical studies. Potentiometric measurements were carried out using a Multimeter (Metrohm, 744). All potential were referenced to a saturated calomel electrode (SCE). The temperature was kept at 25±0.5 °C during the experiments.

Preparation of the bare carbon composite electrode (CCE) The blank carbon ceramic electrode was prepared according to the procedure described by Lev and co-workers [51]. MTMOS, 0.3 mL, 0.45 mL methanol, and 10 μL hydrochloric acid (11 M) as catalyst were mixed for 3 min and 0.3 g carbon powder was added and the resultant mixture shaken for an additional 1 min. The sol–gel carbon mixture was filled in a piece of Teflon tube (7 mm in length and 3.9 mm in inner diameter) and the mixture was then dried overnight under ambient conditions (~25 °C). Electric contact was made with copper wire through the back of the electrode. The electrode were polished with polishing paper and subsequently rinsed with doubly distilled water.

Preparation of α- and β-PbO_2 modified CCEs Two different crystal structures were known for solid PbO_2, α and β. When the electrodeposition of PbO_2 occurs in acidic media, the β form is preferably formed [59], whereas α-PbO_2 is preferably deposited from alkaline solution [60]. The present work describes pH-sensitivity of both α- and β-PbO_2 films which were obtained at the CCE as below procedures.

α-PbO_2 The α-PbO_2 film was electrodeposited at CCE in 0.1 mol/L KOH solution containing 20 mmol/L Pb $(CH_3COO)_2$ by cycling the potential between 0.4 and 0.8 V at 50 mV s^{-1} for 10 min. The PbO_2 film deposited by this procedure is seen as brown color on the CCE. Then the electrode was removed from the solution and rinsed with doubly distilled water.

β-PbO_2 The β-PbO_2 film was electrodeposited at CCE in 0.1 mol/L HNO_3 solution containing 20 mmol/L $Pb(NO_3)_2$ by cycling the electrode potential between 1.2 and 1.6 V at 50 mV s^{-1} for 10 min. The PbO_2 film deposited by this manner is seen as dark teal color on the CCE. Then the electrode was removed from the solution and rinsed with doubly distilled water.

Results and discussion

Electrodeposition of α-PbO_2 film In order to find an optimized potential range for the electrodeposition of PbO_2 film, potential of the CCE in 0.1 mol/L KOH solution containing 20 mmol/L $Pb(CH_3COO)_2$, was cycled between −0.35 and 0.75 V vs. the SCE (Fig. 1a). As can be seen, two anodic current peaks due to oxidation of $Pb^{II} \rightarrow Pb^{IV}$ appeared at 0.57 and 0.69 V, respectively; where the current peak at less positive potential may be attributed to the case that the reaction product adsorbed at the electrode surface, making a facility in electrode process. Similarly, two cathodic current peaks due to the reduction of $Pb^{IV} \rightarrow Pb^{II}$ were recorded at 0.18 and 0.0 V, respectively; where, the peak current at less negative potential may be attributed to the reduction of free Pb^{IV} species, and the other one at 0.0 V may be related to the reduction of Pb^{IV} previously adsorbed to the electrode surface. Based on these observations, we concluded that the Pb^{IV} as α-PbO_2 film can be deposited on the CCE by the repetitive potential scanning in the range of 0.4–0.8 V, for which, only flat anodic currents for both

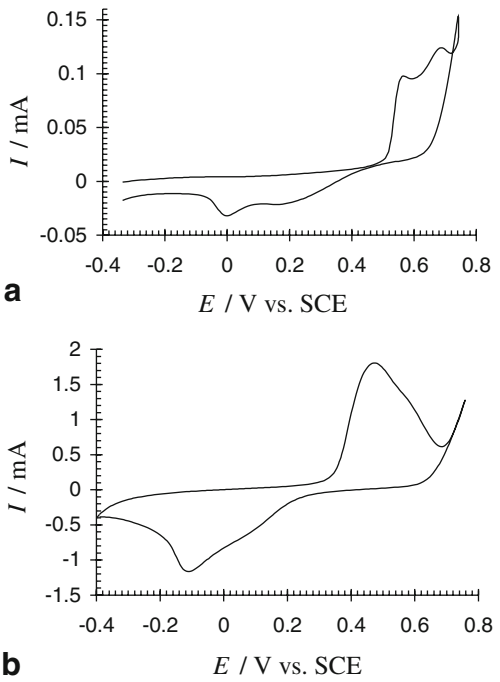

Fig. 1 (**a**) Cyclic voltammogram of the CCE in 0.1 M KOH solution containing 20 mM $Pb(CH_3COO)_2$ at a scan rate of 50 mV s^{-1}. (**b**) Cyclic voltammogram of the same CCE after coating α-PbO_2 film, recorded in 0.1 M KOH solution at scan rate of 50 mV s^{-1}

positive and negative scans were observed in the stirred solution (figure not shown). By cycling the electrode potential for a 10-min period of time, α-PbO_2 film (brown color) was formed on the CCE.

Figure 1b shows the cyclic voltammogram of α-PbO_2-film-modified CCE in 0.1 mol/L KOH solution containing no deliberately added $Pb(CH_3COO)_2$. As can be seen, the voltammetric behavior of PbO_2-coated CCE differs from that observed at CCE in $Pb(CH_3COO)_2$ solution. The appearance of current peaks deals with the attachment of lead dioxide film on the electrode surface. It may be pointed out that the anodic and cathodic peaks consist of two overlapped peaks. The surface reactions due to redox peaks may be shown as follows:

$$PbO_2 + H^+ + e^- \rightleftharpoons PbOOH \quad (1)$$

$$PbOOH + H^+ + e^- \rightleftharpoons PbO + H_2O \quad (2)$$

A similar experiment was carried out to optimize potential range required for electrodeposition of β-PbO_2. It was found that the β-PbO_2 film can firmly be electrodeposited at CCE in 0.1 mol/L HNO_3 solution containing 20 mmol/L $Pb(NO_3)_2$ by cycling the electrode potential between 1.2 and 1.6 V at 50 mV s^{-1} for 10 min.

pH-sensing theory The initial behavior of the α- and β-PbO_2 electrodes was close to that predicted by a number of electrochemical equilibria. General mechanisms which describe the response of metal oxides to pH are proposed by Fog and Buck [43] and Liu et al. [61]. These involve a potentiometric pH response caused by either equilibrium between two solid phases of the oxide or the intercalation of species into the oxide structure. Since the PbO_2 electrode is treated as pH electrode, the internal redox reactions can be represented as Eq. (1). In this case, the Nernst equation can be written as:

$$E = E^\circ + \frac{RT}{F} \ln \frac{a_{PbO_2} a_{H^+}}{a_{PbOOH}} \quad (3)$$

Assuming a constant value for (a_{PbO_2}) and (a_{PbOOH}) in the solid film, Eq. (3) can be expressed as:

$$E = \frac{RT}{F} \ln a(a_{H^+}) + \text{constant} \quad (4)$$

Where (a_{H^+}) is the proton activity in the liquid phase; at 25 °C, the Eq. (4) can be shown as:

$$E = \text{constant} - 0.05916\text{pH} \quad (5)$$

According to Eq. (5), a plot of the measured emf (E) vs. pH should yield a straight line with a slope of −59.16 mV/pH unit at 25 °C. As can be seen from Fig. 2, the proposed pH sensors based on α- and β-PbO_2 are sensitive to the pH variations and show linear behavior over a wide pH range of 1.5–12.5 at room temperature with a near-Nernstian slope of −64.82 and −57.85 mV/pH unit, respectively.

The potentiometric signals measured with both modified electrodes reached stable values very rapidly. After, when the electrode response reached steady state, a tiny change in signals was observed for hours, reinforcing the utility of the sensor for routine analysis. The response time as well as dynamic pH range was improved at the proposed pH sensor with respect to some approaches based on similar metal oxides and conducting polymers. The sensitivity and dynamic pH range achieved for PbO_2|CCE and some non-glass pH sensors were comparatively summarized in Table 1.

The reproducibility of the sensor preparation procedure is an important key that must be considered. In order to validate sensor preparation procedure, the PbO_2|CCE was repetitively prepared for five times and each electrode was tested in term of pH sensitivity (slope of E vs. pH plot) and $E^{0\prime}$ (extrapolated formal potential at zero pH). According to Fig. 3, all the sensors appeared linear response to pH changes in a relatively wide pH range. A statistical treatment was carried out on data concerning the slopes (s) and intercepts (h) obtained from regression lines. The slope and intercept are important characteristics indicating the efficiency of a potentiometric sensor. Therefore, we evaluated our proposed sensor preparation method by calculating the RSD (%) values that were found to be 3.23% and 2.26% for slope and intercept, respectively.

Step-change response The response time of β-PbO_2 sensor for step-change in solution pH was studied at hydrodynamic conditions. An experiment was designed for which the solution pH was frequently changed from 12 to 2 and vice versa. Generally, the response to step-change in pH in both

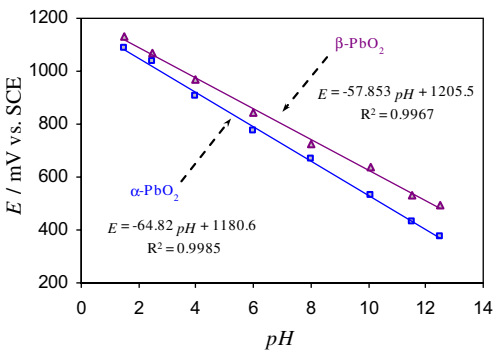

Fig. 2 Potentiometric responses to pH changes of α-PbO_2 (*filled square*) and β-PbO_2-(*filled upright triangle*) film-modified CCE electrodes in phosphate buffer solutions of 0.1 M

Table 1 The major characteristics of some non-glass pH sensors

Electrode material	Slope (mV/decade)	Response time	pH range	Log $K^{pot}_{H,M}$	Ref.
Single crystals of molybdenum bronzes	~(−60)	5 s for 90%	3–9	–	[47]
Ruthenium dioxide	−52.1	10 min	2–10	–	[38]
MnO_2-montmorillonite composite	−55.0	2 min	1.6–12.5	–	[48]
Nano-sized cobalt oxide	−56.4	Less than 1 min	1–12	Li^+: – Na^+: <−12 K^+: <−12 Ca^{2+}: <−12	[50]
Sol–gel derived (xerogel) based on covalently attached amine groups	−55	≤3 s	3–8	Li^+: – Na^+: −13 K^+: −11 Ca^{2+}: –	[62]
Iridium oxide on Ti substrates	−73.7	1 min	1.5–11.5	–	[63]
Poly 3,4-dihydro-2-hydroxyquinooxaline thin film modified with Pt nanoparticles	−63.3	Several seconds at pH 7, 2.5 min at pH 13	2–12	–	[64]
PbO_2–paraffin matrix on graphite	−100	A few seconds	1.2–7.5	–	[45]
Polyaniline on carbon fiber	−60	Several sec at pHs around 7 up to 2 min at pH 12.5	2.0–12.5	Li^+: −12 Na^+: −12.1 K^+: −11.9 Ca^{2+}: −11.6	[5]
Graphite/quinhydrone composite	−57.6	3–5.4 s	2–8	–	[22]
Quinhydrone composite	−57.3	5	2–8	–	[21]
Hydroquinone-Functionalized Polypyrrole	−46	6 min	3–10	–	[18]
Polypyrrole films	−27 to −51	Less than 2 min	2–11	–	[10]
Lead dioxide films on CCE	α: −64.82	pH<7: ~1 s	1.5–12.5	Li^+: −12.21 Na^+: −12.31	This work
	β: −57.85	pH>7: 30 s		K^+: −12.29 Ca^{2+}: −12.58	

directions was reasonably fast. The responses in the two directions, as shown in Fig. 4, were markedly different.

The addition of acid to an alkali buffer caused a very sharp change in open circuit potential measured with 0.3 s intervals. For all electrodes, the time needed for 90% response (t_{90}) was calculated to be about 1 s. However, considering the solution-mixing effects, the response is actually much faster than this value.

The step from acid to alkali regions is in the form of a smooth curve. The measured potential continues to fall slowly during the 170 s after KOH addition. For PbO_2| CCE, t_{90} was calculated to be about 30 s. It is possible that there is a surface reaction with the alkali which modifies the pH response. This reaction takes place relatively slowly resulting in the gradual drop in potential observed in this

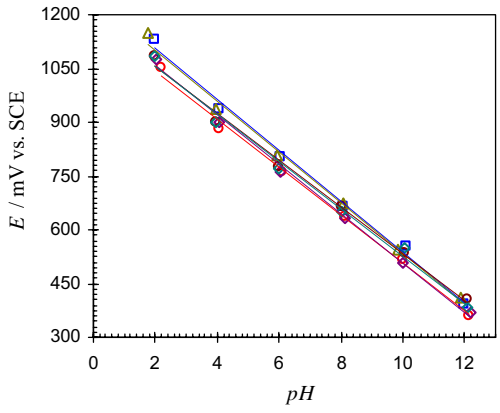

Fig. 3 Potentiometric responses to pH changes of α-PbO_2-film-modified CCE electrodes (repetitively prepared for 5 times) in phosphate buffer solutions of 0.1 M

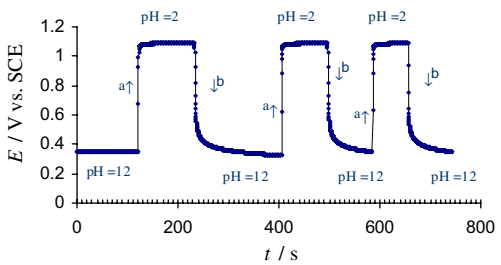

Fig. 4 Potentiometric response of β-PbO_2 sensor to downward (**a**) and upward (**b**) pH steps

case. To the authors, the proton separation or abstraction was probably slow and the limiting factor. As a result, the 30-s equilibration time was not thought to be adequate enough to ensure a stable reading in high pH buffers by the PbO_2|CCE. However, the electrode potential is completely stabilized during 1 s in acidic medium. The PbO_2 sensor with t_{90} times of less than 1 min in both cases could have practical applications in many areas.

Long-term stability and repeatability The long-term stability of the PbO_2 pH sensor was investigated for a 60-day period of time under constant experimental conditions (i.e., pH 2, 0.1 M phosphate buffer). Figure 5 shows the variations in potential response of the α- and β-PbO_2 pH sensor versus the elapsed time. According to Fig. 5, the pH sensors presented a high level stability during long-term usage. In addition, the electrode shows nearly constant sensitivity (Nernstian slope) for a period of 2 months when it was kept in air or partially used to test. A mean value of 4.5 mV as a drift in slope (sensitivity) was found for five electrodes examined. The stability of the pH sensors is mainly related to the persisting attachment of PbO_2 film with the CCE surface or electrochemical properties of metal oxides improved at the carbon composite electrode. In contrast, the electrode sensitivity was decreased in the case of full operation in complex matrices containing iodide, I^-, citrate, $C_6H_5O_7^{3-}$, ions such as some fruit juices. In these matrices, a freshly prepared electrode can be used for 2 weeks. This limitation mustn't be considered serious because of easy and fast preparation a new PbO_2 film on CCE.

In order to weigh up the efficiency of calibration-free PbO_2 pH sensor in potentiometric titrations and estimation of its repeatability, the titration of acetic acid with potassium hydroxide was selected as a model and it was repetitively carried out for four times and the end point was monitored by using α- and β-PbO_2|CCE electrode. The results obtained for the case of α-PbO_2|CCE were shown in Fig. 6. The relative standard deviation (RSD) for the end point determination of titrations was found to be 0.296% and 0.468% for α- and β-PbO_2 electrodes, respectively. Also repeatability of the pH sensors for direct measurements of the solutions pH was evaluated. To do that, ten successive measurements in pH 2 was carried out by two kinds of electrodes. The RSD values were calculated as 0.214% and 0.673% for α- and β-PbO_2 electrodes, respectively. These results make the proposed pH sensor attractive for analytical applications both in direct and indirect measurements.

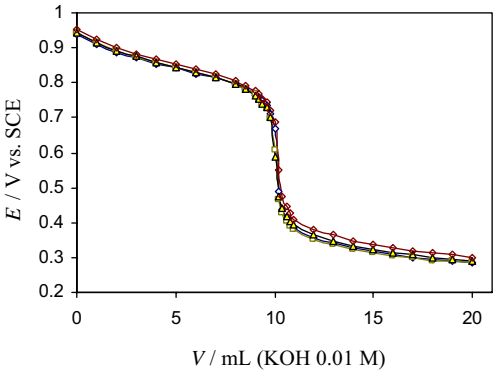

Fig. 6 Four repetitive titration curves obtained for 10 mL acetic acid solution (~0.01 M), by standard potassium hydroxide solution of 0.01 M, using α-PbO_2|CCE

Influence of coexisting some possible interfering ions Considering Eq. (1), it seems that some metallic cations especially alkali-cations may cause an electrochemical interference. The effect of some cations on the potentiometric response of the proposed pH sensor was studied based on fixed interference method (FIM). The emf of a cell comprising PbO_2|CCE and SCE reference electrode (ISE cell) is measured with solutions of constant activity of interfering cation, a_M, and varying activity of the primary H^+ ion. The emf values obtained are plotted vs. the logarithm of the activity of the H^+ ion (a_{H^+}) as shown in

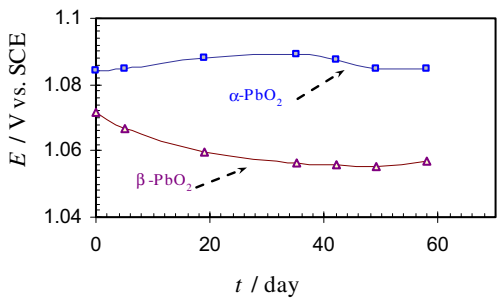

Fig. 5 Stability of potentiometric response of α-PbO_2 (*filled square*) and β-PbO_2-(*filled upright triangle*) film-modified CCE electrodes for period of 60 days

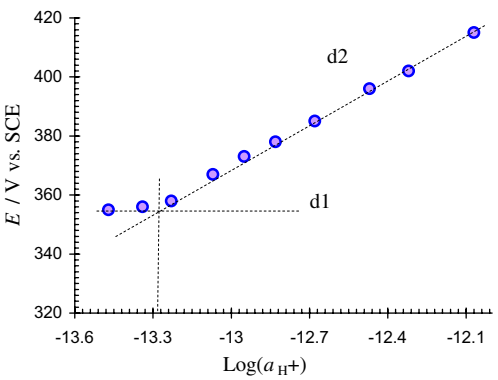

Fig. 7 Determination of potentiometric selectivity coefficient $K^{pot}_{H,M}$, for cation K^+ (0.1 M in solution) with respect to the principal ion H^+ at β-PbO_2|CCE as pH sensor

Table 2 The potentiometric selectivity coefficient for cation M^{n+} with respect to the principal ion H^+, found for PbO_2|CCE as pH sensor

Interfering species	$-\text{Log } K^{pot}_{H,M}$ at α-PbO_2	$-\text{Log } K^{pot}_{H,M}$ at β-PbO_2
K^+	12.28	12.29
Na^+	12.40	12.31
Li^+	12.04	12.21
Ca^{2+}	12.43	12.58

Fig. 7. The intersection of the extrapolation of the linear portions of this plot (lines d1 and d2 in Fig. 7) indicates the value of a_{H^+} which is to be used to calculate $K^{pot}_{H,M}$ from the Nikolsky–Eisenman equation [65]:

$$E = \text{constant} + \frac{2.303RT}{z_A F} \times \log\left[a_A + K^{pot}_{A,B} a_B^{z_A/z_B} + K^{pot}_{A,C} a_C^{z_A/z_C} + \ldots\right] \quad (6)$$

$$K^{pot}_{A,B} = \frac{a_A}{a_B^{z_A/z_B}} \quad (7)$$

Where, $K^{pot}_{A,B}$ is the potentiometric selectivity coefficient for ion B with respect to the principal ion A; $a_A$and a_B are the activity of the primary ion (a_{H^+}) and interference ion. The potentiometric selectivity coefficient for some cations at PbO_2 pH sensor was calculated and the results are presented in Table 2. The values obtained for $K^{pot}_{H,M}$ are comparable with that reported on solid-state pH nano-electrode based on polyaniline thin film [5].

Unlike cations, the anions may be cause chemical interferences via two different mechanisms: (1) some anions interact with the H^+ ion being measured then decreases its activity. The sensor continues to report the true activity while a considerable gap occurs between the

Table 3 Estimation of relative error (%) on potentiometric response of α- and β-PbO_2 pH sensors in pH 7 (PBS 0.1) caused by interfering anions at concentration level of 2×10^{-3} M

Interfering species	Relative error for α-PbO_2	Relative error for β-PbO_2
F^-	2.11	1.79
Cl^-	2.15	0.69
Br^-	2.85	0.73
I^-	6.20	6.18
HCO_3^-	2.57	2.31
SO_4^{2-}	3.27	1.72
CH_3COO^-	1.9	1.92
$C_6H_5O_7^{3-}$	3.9	2.08
NO_3^-	1.99	0.21

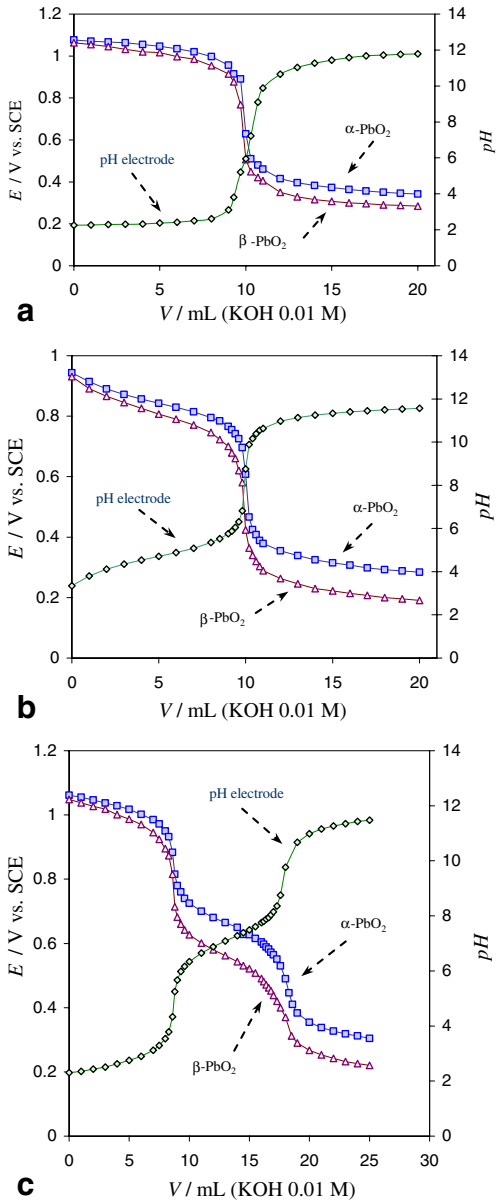

Fig. 8 Titration curve of 10 mL hydrochloric acid (**a**), acetic acid (**b**) and phosphoric acid (**c**) solutions (~0.01 M) by standard potassium hydroxide solution of 0.01 M, using α-PbO_2 (*filled square*), β-PbO_2 (*filled upright triangle*) electrodes and a conventional glass pH electrode (*filled diamond*)

Table 4 The results obtained for determination of pH in some real samples by glass pH electrode and proposed α- and β-PbO_2 pH sensors

Real samples	The measured pH		
	Glass electrode	α-PbO_2[a]	β-PbO_2[a]
Lemon juice	2.47	2.84±0.33	2.21±0.65
Orange	3.12	3.35±0.32	2.86±0.57
Vinegar	2.82	2.91±0.34	2.83±0.57
Apple	3.26	3.21±0.32	3.21±0.54

[a] Each result is average of five replicate measurements.

activity and apparent concentration of H^+. Under these circumstances, the determination of ionic concentration may be problematic. (2) Other anions may be interacting with the membrane itself, blocking the surface or changing its chemical composition or poisoning electrode.

The interfering effects of a series of anions on the response PbO_2 pH sensor were investigated. The sensor response was nearly independent of some anions examined. The slight changes in sensor response caused by some anions evaluated and the results are presented in Table 3. Among the anions, citrate and iodide could make a considerable interference effect (below 7%) on the sensor response.

In the present study, the α- and β-PbO_2 pH sensors showed the similar stability, repeatability, and pH-sensing property; however, they were differently affected by interfering ions, i.e., the relative error calculated in the case of β-PbO_2 is less than that of α-PbO_2. The reason for this behavior may be strongly related to the difference between the crystal structures of α- and β-PbO_2. Wherein α-lead dioxide has the orthorhombic structure of columbite and β-lead dioxide has the tetragonal rutile structure [66].

Analytical applications In order to evaluate the utility of proposed pH sensor to monitoring acid–base titrations in aqueous solution, a number of acid–base titrations were carried out. To do that, a strong acid, a weak acid, and a poly-protic acid were chosen as typical of examples. Figure 8 shows the potentiometric titration curves for hydrochloric, acetic, and phosphoric acid solutions (~0.01 M) by standard potassium hydroxide solution (0.01 M). In order to compare the results, a parallel titration was also carried out using a glass pH electrode and experimental data were shown in Fig. 8. It is clear that both α- and β-PbO_2|CCEs show the same behavior in acid–base titrations, and the end-points in the all titration curves are very close together. In addition, it is worth noting that for such dynamic measurements, the response time of both modified electrodes falls below 20 s.

In order to evaluate the efficiency of the proposed sensor for measuring the pH in complex matrixes, a number of real samples were tested. The pH values were obtained using interpolation from a calibration *E* vs. pH plot. As seen in Table 4, the results obtained by the proposed pH sensor and glass electrode are in good agreement (with a maximum difference of 0.26 pH unit except lemon juice). In the case of lemon juice, the main interfering effect can be related to the presence of citrate ions $\left(C_6H_5O_7^{3-}\right)$ in this sample because our preliminary study has showed that the citrate ions could make a considerable interference effect on the sensor response (Table 3). We derived a statistical treatment on the results obtained by using PbO_2|CCE sensors and glass pH electrode; No systematic error was found at a confidence level of 95%.

Conclusions

The present paper described the use of CCE as a novel active surface for electrodeposition of PbO_2 films with different crystal structures named α and β. The PbO_2 film showed an excellent response time, high selectivity, good stability, pH sensitivity, and long-term usage due to its persisting attachment with CCE surface. Both modified electrodes exhibit a near-Nernstian behavior in the pH range 1.5–12.5. The PbO_2-coated CCE was used as a pH sensor for monitoring of acid–base titration, measuring of the pH in lab-made solutions, as well as real samples such as apple juice, orange juice, etc. In all cases, a satisfactory agreement was observed between the results obtained at PbO_2|CCE and a conventional glass pH electrode.

References

1. Severinghaus JH, Astrup PB (1985) J Clin Monit 1:180
2. Peterson JI, Goldstein SR, Fitzgerald RV, Buckhold DK (1980) Anal Chem 52:864
3. Grant SA, Glass RS (1997) Sens Actuators B 82:35
4. Rodrigues Jr JJ, Barbosa Neto NM, Balogh DT, Zilio SC, Misoguti L, Mendonca CR (2003) Opt Commun 216:233
5. Xueji Z, Ogorevc B, Wang J (2002) Anal Chim Acta 452:1
6. Heieman WR, Wieck HJ, Yacyaych AM (1980) Anal Chem 52:345
7. Cheek G, Wales CP, Owak RJ (1983) Anal Chem 55:380
8. Noboru O, Tomoaki H, Shuichiro Y (1983) Anal Chem 59:258
9. Yuan R, Chai YQ, She GL, Yu RQ (1993) Talanta 40:1255
10. Lakard B, Segut O, Lakard S, Herlem G, Gharbi T (2007) Sens Actuators B 122:101
11. Lakard B, Herlem G, Lakard S, Guyetant R, Fahys B (2005) Polymer 46:12233
12. Rayss J, Sudolski G (2002) Sens Actuators B 87:397
13. Lehmann H, Schwotzer G, Czerney P, Mohr GJ (1995) Sens Actuators B 29:392
14. Sharma NK, Gupta BD (2003) Opt Commun 216:299
15. Meites L, Thomas HC (1958) Advanced Analytical Chemistry. McGraw-Hill, New York Chap. 4
16. Lingane JL (1958) Electroanalytical Chemistry. Interscience, New York Chap. 4
17. Meites L, Bates RG, Bower VE (1963) Handbook of Analytical Chemistry. McGraw-Hill, New York Section 11
18. Aquino-Binag CN, Kumar N, Lamb RN, Pigram PJ (1996) Chem Mater 8:2579
19. Düssel H, Komorsky-Lovric Š, Scholz F (1995) Electroanalysis 7:889
20. Kahlert H (2002) In: Scholz F (ed) Electroanalytical Methods—Guide to Experiments and Applications. Springer, Heidelberg
21. Kahlert H, Steinhardt T, Behnert J, Scholz F (2004) Electroanalysis 16:2058
22. Kahlert H, Pörksen JR, Isildak I, Andac M, Yolcu M, Behnert J, Scholz F (2005) Electroanalysis 17:1085
23. Herlem G, Goux C, Fahys B, Dominati F, Gonçalves A-M, Mathieu C, Sutter E, Trokourey A, Penneau J-F (1997) J Electroanal Chem 435:259
24. Nyholm L, Peter LM (1994) J Chem Soc Faraday Trans 90:149
25. Karyakin AA, Vuki M, Lukachova LV, Karyakina EE, Orlov AV, Karpachova GP, Wang J (1999) Anal Chem 71:2534

26. Karyakin AA, Lukachova LV, Karyakina EE, Orlov AV, Karpachova GP (1999) Anal Commun 36:153
27. Talaie A (1997) Polymer 38:1145
28. Sergeyeva TA, Lavrik NV, Piletsky SA, Rachkov AE, Elskaya AV (1996) Sens Actuators B34:283
29. Lindfors T, Ivaska A (2000) Anal Chim Acta 404:111
30. Erdogdu G, Karagozler AE (1997) Talanta 44:2011
31. Cho WJ, Huang HJ (1998) Anal Chem 70:3946
32. Chaubey A, Pande KK, Singh VS, Malhotra BD (2000) Anal Chim Acta 407:97
33. Liu CH, Liao KT, Huang HJ (2000) Anal Chem 72:2925
34. Tarlov MJ, Semancik S, Kreider KG (1990) Sens Actuators B1:293
35. Pasztor K, Sekiguchi A, Shimo N, Kitamura N, Masuhara H (1993) Sens Actuators B12:225
36. Olthuis W, Robben MA, Bergveld P, Bos M, Avn Der Linden WE (1990) Sens Actuators B2:247
37. Hendrikse J, Olthuis W, Bergveld P (1998) Sens Actuators B53:97
38. Mihell JA, Atkinson JK (1998) Sens Actuators B48:505
39. Lambrechts M, Sansen W, Suls J, Paszczynski S (1988) Sens Actuators 13:287
40. Pasztor K, Sekiguchi A, Shimo N, Kitamura N, Masuhara H (1993) Sens Actuators B13–14:561
41. McMurray HN, Douglas P, Abbott D (1995) Sens Actuators B28:9
42. Liao Y-H, Chou J-C (2008) Sens Actuators B128:603
43. Fog A, Buck RF (1984) Sens Actuators 5:137
44. Kinoshita K, Madou MJ (1984) J Electrochem Soc 131:1089
45. Lima AC, Jesus AA, Tenan MA, de Souza Silva AF, Oliveira AF (2005) Talanta 66:225
46. Arshak K, Gill E, Arshak A, Korostynska O (2007) Sens Actuators B127:42
47. Shuk P, Ramanujachary KV, Greenblatt M (1996) Electrochim Acta 41:2055
48. Tellia L, Brahimia B, Hammouche A (2000) Solid State Ionics 128:255
49. Qingwen L, Yiming W, Guoan L (1999) Sens Actuators B 59:42
50. Qingwen L, Guoan L, Youqin S (2000) Anal Chim Acta 409:137
51. Tsionsky M, Gun G, Glezer V, Lev O (1994) Anal Chem 66:1747
52. Lev O, Tsionsky M, Rabinovich L, Glezer V, Sampath S, Pankratov I, Gun J (1995) Anal Chem 67:22A
53. Wang J, Pamidi PVA, Rogers KR (1998) Anal Chem 70:1171
54. Collinson MM, Howells AR (2000) Anal Chem 72:702A
55. Rabinovich L, Lev O (2001) Electroanalysis 13:265
56. Gun G, Tsionsky M, Lev O (1994) Anal Chim Acta 294:261
57. Pamidi PVA, Parrado C, Kane SA, Wang J, Smith MR, Pingarrón JM (1997) Talanta 44:1929
58. Dunn B, Farrington GC, Katz B (1994) Solid State Ionics 70–71:3
59. Ueda M, Watanabe A, Kameyama T, Matsumoto Y, Sekimoto M, Shimamune T (1995) J Appl Electrochem 25:817
60. Rüetschi P, Angstadt RT, Cahan BD (1959) J Electrochem Soc 106:547
61. Liu CC, Bocchiccio BC, Overmyer PA, Neuman MR (1980) Science 207:188
62. Marxer SM, Schoenfisch MH (2005) Anal Chem 77:848
63. Marzouk SAM (2003) Anal Chem 75:1258
64. Li X, Zhang Z, Zhang J, Zhang Y, Liu K (2006) Microchim Acta 154:297
65. Buck RP, Lindner E (1994) Pure Appl Chem 66:2527
66. Carr JP, Hampson NA (1972) Chem Rev 72:6